

ChemComm

Accepted Manuscript



This is an *Accepted Manuscript*, which has been through the Royal Society of Chemistry peer review process and has been accepted for publication.

Accepted Manuscripts are published online shortly after acceptance, before technical editing, formatting and proof reading. Using this free service, authors can make their results available to the community, in citable form, before we publish the edited article. We will replace this *Accepted Manuscript* with the edited and formatted *Advance Article* as soon as it is available.

You can find more information about *Accepted Manuscripts* in the [Information for Authors](#).

Please note that technical editing may introduce minor changes to the text and/or graphics, which may alter content. The journal's standard [Terms & Conditions](#) and the [Ethical guidelines](#) still apply. In no event shall the Royal Society of Chemistry be held responsible for any errors or omissions in this *Accepted Manuscript* or any consequences arising from the use of any information it contains.

Cite this: DOI: 10.1039/c0xx00000x

www.rsc.org/xxxxxx

ARTICLE TYPE

A New Strategy for Synthesis of Porous Magnetic Supraparticles with Excellent Biodegradability

Dian Li,^a Yuting Zhang,^a Meng Yu,^a Qiao An,^a Jia Guo,^a Jennifer Q Lu^b, Changchun Wang^{*a}

Received (in XXX, XXX) Xth XXXXXXXXXX 20XX, Accepted Xth XXXXXXXXXX 20XX

DOI: 10.1039/b000000x

Porous magnetic supraparticles (p-MSPs) with surface area up to 285.4 m²/g have been fabricated by a one-step etching method that is 4 times greater than the unetched counterpart. They exhibit significantly better biodegradability than its counterpart in both mimicked physiological buffer solution and the cellular environment of HeLa cells.

Benefiting from extremely high porosity and the ability to tune pore size, porous nanomaterials including mesoporous titanium dioxide (m-TiO₂),^{2a} mesoporous silica (m-SiO₂),^{2b,2c} porous carbon,^{2d} covalent organic frameworks (COF)^{2e} and metal-organic frameworks (MOF)^{2f} have been exploited for various applications.^{1,2,3} This includes serving as vehicles or reservoirs for drug delivery,^{3a,3b} as adsorbents^{3c-3e} and heterogeneous catalysts or catalyst support.^{3f}

Recently, we have pioneered a solvothermal-based method to synthesize sub-micron-sized mesoporous Fe₃O₄ colloidal nanocrystal clusters, named as magnetic supraparticles (MSPs).⁴ During the synthesis procedure, polymer-stabilized magnetic supraparticles co-assemble with the polymer stabilized gas bubbles to form the nanocrystal clusters. The pores are in-situ formed without the need of adding materials.^{4b} Moreover, the MSPs that are composed of iron oxides can be degraded in acidic medium simulating the tumour cellular environment and endosome,^{4b, 4c} as what we previously reported.⁵ This MSP synthesis method can provide an effective albeit limited controllability of pores. Furthermore enhancement of porosity and adjustment of pore size remain elusive.

Herein, we report a new strategy to generate porous MSPs (p-MSPs) by utilizing the etching properties of a DMF solution of methyl mercaptoacetate that is a complexing agent, and hydrazine which is a reducing agent. The Fe₃O₄ component of MSPs can be reduced gradually by hydrazine to form Fe(OH)₂, which will be coordinated with methyl mercaptoacetate to dissolve in DMF. As a result, the interspaces will be increased as well as the porosity of the MSPs. The as-prepared p-MSPs possess unusually larger pore volume and surface area than its counterpart without this additional etching step. They show higher acidic degradation rate and have the potential to be applied in delivery and storage of guest molecules.

As previously reported, the MSPs stabilized by agarose possess solid inner and roughened surfaces (Fig. 1a). However, when we added the MSPs into the DMF solution containing hydrazine, a reducing agent, and methyl mercaptoacetate, a chelating agent, to

react with MSPs at 80 °C, the structure of the MSPs are clearly changed. After reaction for 30 min, some new interspaces appear in the MSPs (Fig. 1b). With gradual increase of the reaction time, the interspaces in MSPs became more and more noticeable. This is as evidenced by greater numbers of tortuous channels that are generated in the MSPs after 60-min reaction (Fig. 1d). If the reaction time is allowed to continue, the skeleton of the MSPs is broken down after 120 min (Fig. S1 and S2).

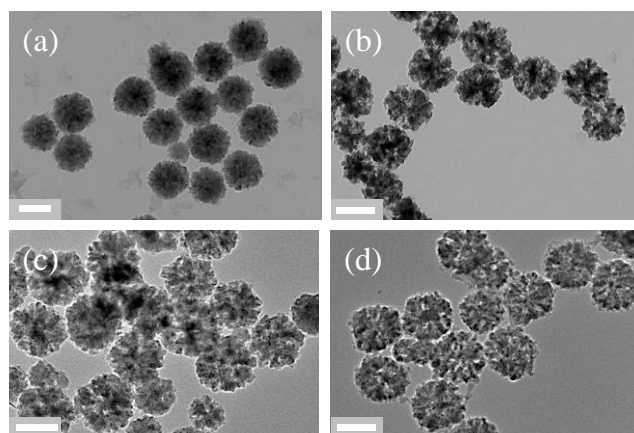


Fig. 1 The TEM images of (a) MSPs stabilized by agarose, the MSPs reacted with hydrazine and methyl mercaptoacetate in DMF for (b) 30 min, (c) 45 min, and (d) 60 min. All the bars are 100 nm.

Table 1 The porous characteristics of p-MSPs prepared by varying the etching time.

Etching time (min)	Surface area (m ² /g) ^[a]	Pore volume (cm ³ /g)
0	55.8	0.15
30	109.6	0.34
45	194.6	0.51
60	285.4	0.77
75	226.7	0.58
120	126.4	0.26

[a] Calculated by the BET method.

Table 1 is a list of surface area and pore volume with reaction time. At the beginning of the reaction, the surface area went up gradually, and reached to the max value of 285.4 m²/g after 60 min., which is significantly greater than that of the precursor MSPs (~58.5 m²/g).^{4c} This result indicates that the generated interspaces indeed could elevate the surface area of MSPs

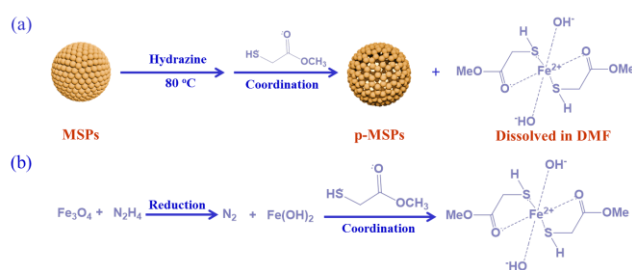
effectively. When the reaction time exceeded 60 min, the surface area of MSPs started to decrease gradually, and the pore volume of the p-MSPs decrease as well. This is because of the skeleton started to collapse. Therefore, by controlling the reaction time, the property of p-MSPs including surface area can be adjusted accordingly.

In addition, with the increase of etching time, the magnetization value of p-MSPs is gradually decreased (Fig. S3). This suggests either the reduction of the amount of magnetite in the particles or possible deterioration of crystallinity p-MSPs that was detected by the PXRD. The PXRD results showed that the crystallization of p-MSPs hardly changed prior to p-MSPs breaking down (Fig. S4a). The TGA results (Fig. S4b) depict that the percentage of stabilizer in whole particle increases along with etching time, implying that the amount of magnetite decreased with the etching time. Moreover, through analysis of the p-MSPs by FT-IR (Fig. S5), we found that the ratio between the C-O peaks (ascribed to carbohydrate chain of agarose)^[4c] at $\sim 1100\text{ cm}^{-1}$ and the C=O (ascribed to the carboxyl group of coordinating with Fe_3O_4)^[4c] peak at $\sim 1600\text{ cm}^{-1}$ increased with longer reaction time. This indicates that the content of Fe_3O_4 in p-MSPs decreased and thus the porosity of p-MSPs increased by etching of Fe_3O_4 in MSPs.

Analyzing the changes of those p-MSPs before and after etching, our hypothesis is that the generation of interspaces in p-MSPs may be ascribed to the loss of surface Fe_3O_4 due to the reduction of Fe(III) to Fe(II) by hydrazine. The Fe(II) then subsequently is coordinated with methyl mercaptoacetate and as a result Fe_3O_4 will be removed, leading to enhanced surface area. The etching process involves the following two steps (Scheme 1): (1) Hydrazine reduction of Fe_3O_4 nano-crystals to Fe(II); (2) The sulfhydryl group coordinated with Fe(II) to promote the dissolution in DMF. It is known that methyl mercaptoacetate is a better complexation agent toward Fe(II) than Fe(III),^{6a} and hydrazine as a strong reducer that can easily reduce Fe(III) to Fe(II).⁷ Since hydrazine can reduce Fe_3O_4 to Fe(II) rapidly, and the product Fe(II) can be coordinated with methyl mercaptoacetate in DMF, Fe_3O_4 in MSPs will be etched.

We noticed that as the amount of complexing agent or reductant reduces to zero in the reaction system, the porous structure cannot be generated in the MSPs (Fig. S6 and Fig. S7). Moreover, if the hydrazine was substituted with ethanediamine, which is not a reducing agent but has two amine groups, the MSPs were not etched to p-MSPs as well (Fig. S8). These two pieces of evidence support that the reduction from Fe(III) to Fe(II) by hydrazine is an important step.

We also found some non-magnetic black powders were produced in addition to the p-MSPs. The XPS (Fig. S9) of the black powder showed the Fe peaks are Fe(II) and the peaks of S are ascribed to H-S bond and Fe-S bond.^{6b, 6c} This supports that Fe(II) was indeed reduced and was coordinated with sulfhydryl. Furthermore the PXRD data (Fig. S10) of non-magnetic black powder indicates that the Fe(II) complex was amorphous. These observations led to the conclusion that the etching process is achieved by hydrazine together with methyl mercaptoacetate gradually peeling off the skin of Fe_3O_4 nanocrystals in MSPs to generate the void space.



Scheme 1 (a) The etch mechanism of p-MSP in the presence of hydrazine and methyl mercaptoacetate; (b) The chemical reactions schemes of etching process.

One of the important applications of porous magnetic nanomaterials is drug delivery. We studied the degradation of p-MSPs in acidic medium. As shown in Fig. 2, with the increase of the etching time, the degradation rate of p-MSPs in pH=5.0 buffer increased significantly as evidenced by the greater amount of Fe dissolved in pH5 buffer solution for p-MSP samples etched for longer time. Compared with the MSPs, the p-MSPs etched for 60 min showed a much faster degradation rate. The p-MSPs etched for 60 min could be degraded completely after 180-h incubation whereas only 40 wt % was dissolved for MSPs. This result can be attributed to the combination of faster diffusion rate of acid into the interspaces of p-MSPs, with faster dissolution rates due to the active surface formed after hydrazine/methyl mercaptoacetate etching. Therefore, the formation of interspaces through etching will improve the acidic degradation of p-MSPs.

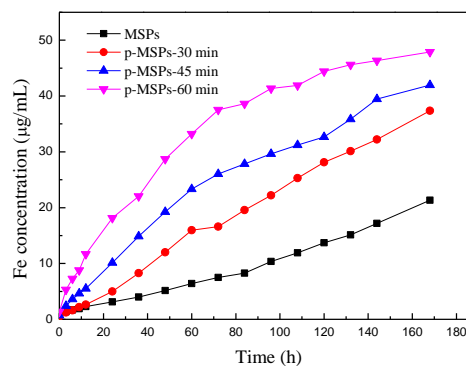


Fig. 2 The curves of the concentration of Fe that dissolved from p-MSPs etched by different time vs co-incubation time in pH=5.0 buffer.

To further investigation of the biodegradation behavior of p-MSPs, HeLa cells were employed as model cells. Our experiments showed that the p-MSPs are non-cytotoxic (Fig. S11). The selective etching method retained agarose in p-MSPs, the stabilizer, which promote their biocompatibility. After staining with an Fe³⁺ sensitive probe, the distribution of Fe³⁺ (dissolved from p-MSPs) in HeLa cells can be observed by confocal laser scanning microscope (CLSM). In Fig. 3, only small areas of red fluorescence were detected in the cells incubated with MSPs whereas strong red fluorescence was observed in the cells incubated with p-MSPs. The intensity of red fluorescence reflects the concentration of Fe³⁺ in the cells,⁵

indicating faster degradation of p-MSPs. This result demonstrated the p-MSPs with high surface area exhibits enhanced biodegradation ability in HeLa cells, coincided with simulated degradation experiment results in pH=5.0 buffer. Thus, combining high surface area with good acidic degradability, p-MSPs offer great potential to serve as biodegradable drug carriers.

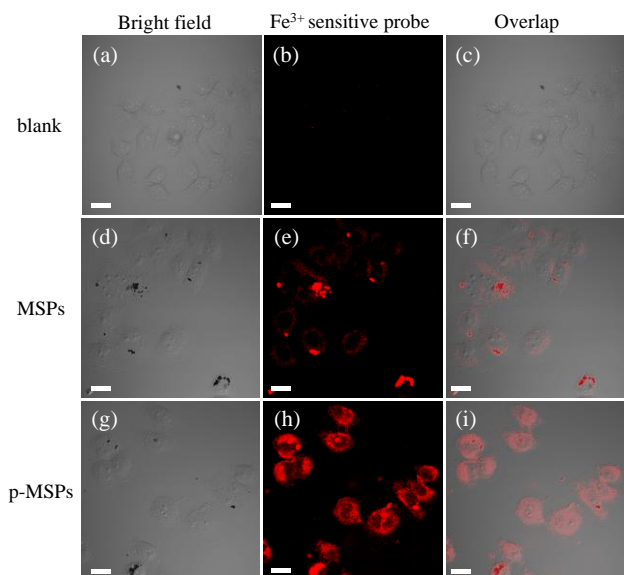


Fig 3 The confocal laser scanning microscope images of MSPs and p-MSPs prepared by 60 min etch of MSPs incubated with HeLa cells for 24 h. The red fluorescence came from the Fe³⁺ sensitive probe combined with Fe³⁺. All the bars were 10 micrometer.

In conclusion, we have synthesized p-MSPs via a one-step etching method of MSPs. p-MSPs stabilized by agarose offer greatly higher porosity in relative to MSPs. Furthermore, the surface area and pore volume can be readily adjusted by etching time. Owing to the extremely large surface area and activated surface, p-MSPs exhibit greatly enhanced acidic degradation capability in both buffer and cellular environment. Since the retainable stabilizer, agarose, can be further modified to endow p-MSPs with more functionalities, we believe that this new system can enable a wide range of applications such as catalysis, separation, and drug delivery.

We acknowledge the financial support of National Science and Technology Key Project of China (Grant No. 2012AA020204); National Science Foundation of China (Grant No 21474017) and Science and Technology Commission of Shanghai (Grant Nos. 13JC1400500 and 13520720200).

Notes and references

^a State Key Laboratory of Molecular Engineering of Polymers, Department of Macromolecular Science, and Laboratory of Advanced Materials, Fudan University, Shanghai, 200433, People's Republic of China. E-mail: ccwang@fudan.edu.cn; Fax: +86-21-65640293

^b Materials Science and Engineering, School of Engineering University of California at Merced Merced, USA. E-mail: jlu5@ucmerced.edu

† Electronic Supplementary Information (ESI) available: Experimental details, TEM images, SEM images, FT-IR spectra, powder X-ray

diffraction data, magnetization data, XPS spectra, TGA and *in vitro* cell assay data. See DOI: 10.1039/b000000x/

- a) J. Andersson, J. Rosenholm, S. Areva and M. Linden, *Chem. Mater.*, 2004, **16**, 4160; b) X. F. Shen, Y. S. Ding, J. Liu, J. Cai, K. Laubernds, R. P. Zenger, A. Vasiliev, M. Aindow and S. L. Suib, *Adv. Mater.*, 2005, **17**, 805; c) A. Walcarius, E. Sibottier, M. Etienne and J. Ghanbaja, *Nat. Mater.*, 2007, **6**, 602; d) J. D. Ryckman, M. Liscidini, J. E. Sipe and S. M. Weiss, *Nano Lett.*, 2011, **11**, 1857. e) A. Walcarius, *Chem. Soc. Rev.*, 2013, **42**, 4098.
- a) J. H. Pan, Z. Y. Cai, Y. Yu and X. S. Zhao, *J. Mater. Chem.*, 2011, **21**, 11430; b) C. H. Lee, L. W. Lo, C. Y. Mo and C. S. Yang, *Adv. Funct. Mater.*, 2008, **18**, 3283; c) S. H. Wu, C. Y. Moua and H. P. Lin, *Chem. Soc. Rev.*, 2013, **42**, 3862; d) Y. D. Xia, Z. X. Yanga and R. Mokaya, *Nanoscale*, 2010, **2**, 639; e) J. Guo, Y. H. Xu, S. B. Jin, L. Chen, T. Kaji, Y. Honsho, M. A. Addicoat, J. Kim, A. Saeki, H. Ihee, S. Seki, S. Irle, M. Hiramoto, J. Gao and D. L. Jiang, *Nat. Commun.*, 2013, **4**, 2736. f) H. L. Jiang and Q. Xu, *Chem. Commun.*, 2011, **47**, 3351.
- a) C. H. Lee, S. H. Cheng, I. Huang, J. Souris, C. S. Yang, C. Y. Mou and L. W. Lo, *Angew. Chem. Int. Ed.*, 2010, **49**, 8214; b) R. J. Xing, A. A. Bhirde, S. J. Wang, X. L. Sun, G. Liu, Y. L. Hou, X. Y. Chen, *Nano Res.* 2013, **6**, 1; c) H. Q. Qin, Z. Y. Hu, F. J. Wang, Y. Zhang, L. Zhao, G. J. Xu, R. A. Wu and H. F. Zou, *Chem. Commun.*, 2013, **49**, 5162; d) Q. Liu, J. Y. Li, H. X. Liu, I. Tora, M. S. Ide, J. W. Lu, R. J. Davis, D. L. Green, J. P. Landers, *Nano Res.* 2014, **7**, 755; e) Y. Zhang, Z. Y. Hu, G. J. Xu, C. Z. Gao, R. A. Wu, H. F. Zou, *Nano Res.* 2014, **7**, 1103; f) Y. Zhang, E. C. Judkins, D. R. McMillin, D. Mehta and T. Ren, *ACS Catal.*, 2013, **3**, 2474.
- a) B. Luo, S. Xu, W. F. Ma, W. R. Wang, S. L. Wang, J. Guo, W. L. Yang, J. H. Hu and C. C. Wang, *J. Mater. Chem.*, 2010, **20**, 7107; b) B. Luo, S. Xu, A. Luo, W. R. Wang, S. L. Wang, J. Guo, Y. Lin, D. Y. Zhao and C. C. Wang, *ACS Nano*, 2011, **5**, 1428; c) D. Li, J. Tang, C. Wei, J. Guo, S. L. Wang, D. Chaudhary and C. C. Wang, *Small*, 2012, **8**, 2690.
- D. Li, Y. T. Zhang, P. Yang, M. Yu, J. Guo, J. Q. Lu and C. C. Wang, *ACS Appl. Mater. Interfaces*, 2013, **5**, 12329.
- a) J. Li, L. Shi, Y. Chen, Y. B. Zhang, Z. G. Guo, B. L. Su and W. M. Liu, *J. Mater. Chem.*, 2012, **22**, 9774; b) S. Shin and J. Jang, *Chem. Commun.* 2007, **43**, 4230; c) G. J. Guan, L. Yang, Q. S. Mei, K. Zhang, Z. P. Zhang and M. Y. Han, *Anal. Chem.*, 2012, **84**, 9492.
- a) M. Kumarraja and K. Pitchumani, *Appl. Catal.*, A 2004, **265**, 135; b) D. Cantillo, M. M. Moghaddam and C. Kappe, *J. Org. Chem.*, 2013, **78**, 4530.